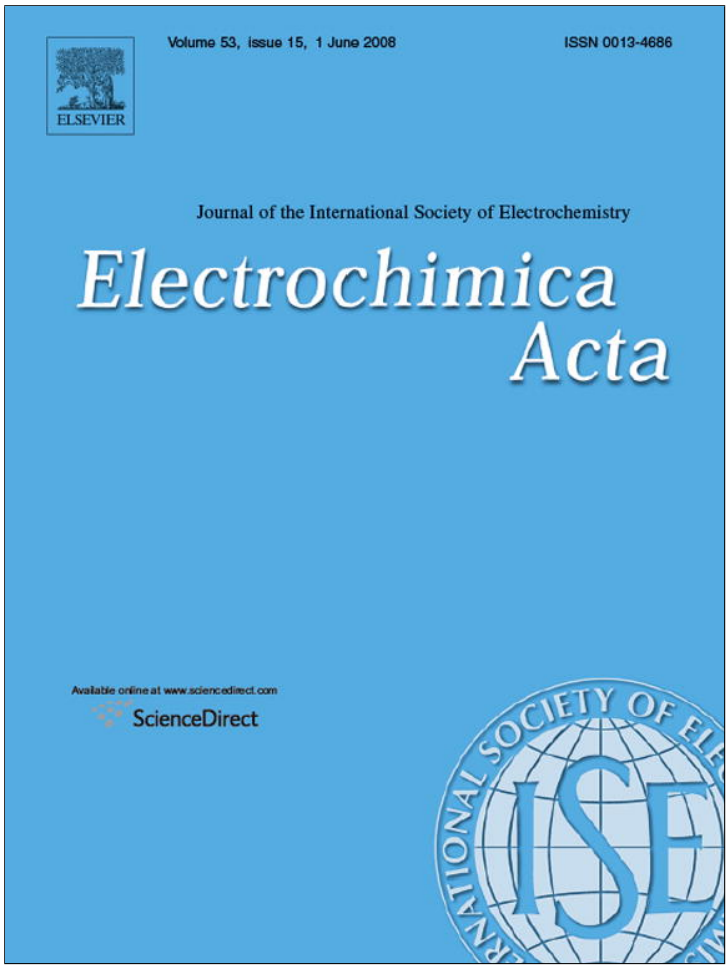

Available online at www.sciencedirect.com
ScienceDirect
Electrochimica Acta 53 (2008) 5007–5015
ELECTROCHIMICA Acta
www.elsevier.com/locate/electacta

Carbon steel passivity examined in alkaline solutions: The effect of chloride and nitrite ions

M.B. Valcarce, M. Vázquez *,[1]

División Corrosión, INTEMA, Facultad de Ingeniería, UNMdP, Juan B. Justo 4302, B7608FDQ Mar del Plata, Argentina

Received 26 October 2007; received in revised form 27 December 2007; accepted 30 January 2008
Available online 9 February 2008

Abstract

The effect of chloride and nitrite ions on the passivity of steel in alkaline solutions was investigated. Four nitrite dosages were tested, resulting in various nitrite/chloride ratios. The behavior of steel was evaluated on electrodes aged during 1 and 90 days, measuring electrochemical parameters such as the corrosion, pitting and repassivation potentials, the corrosion current density, the weight loss and performing electrochemical impedance spectra. The presence of 0.8 mol l^{-1} of chloride induced pitting only under polarization and when the chloride/hydroxyl ratio was not less than one. Nitrite ions behave as effective inhibitors of pit propagation for all the concentrations tested (0.2–0.8 mol l^{-1}). A nitrite/chloride ratio of 0.25 induces complete surface repassivation. Nevertheless, at open circuit potential, the high alkalinity guarantees passivation even in the presence of chlorides. In the event that the passive layer is damaged and pitting can be initiated, nitrite ions are effective in inhibiting pit propagation.

Keywords: Carbon steel; Alkaline solution; Corrosion inhibitor; Chloride; Nitrite

1. Introduction

In reinforced concrete, the bars acting as reinforcements (rebars) are usually low carbon steel bars. The steel is protected against corrosion because concrete provides a highly alkaline environment which guarantees that the metal remains in the passive state. But various contaminants have a detrimental effect on passivity. Among them, chloride ions are the most common ones and localized corrosion triggers when chlorides reach the metal surface. Chloride ions can be incorporated into concrete with seasand, or by using contaminated coarse aggregates, water or additives. Also, being concrete a porous material, chloride ions can penetrate from the atmosphere in structures placed in marine locations. This is certainly the case in many coastal cities in Argentina, where the use of seasand and contaminated aggregates and water constitutes a frequent practice. River sand or "clean" aggregates should be transported from far-away locations and markedly increase the construction costs.

Corrosion of rebars in concrete should be taken seriously from both, the economics and structural integrity standpoints. Many approaches can be used to mitigate the corrosion of reinforcing steel, among which protective coatings and sealers, cathodic protection, concrete realkalinization and corrosion inhibitors are commonly employed. The use of corrosion inhibitors is probably more attractive from the point of view of economics and ease of application [1]. Reviews of the most commonly used corrosion inhibitor types in concrete repair systems and the various possible mechanisms of inhibition have been recently published [2–4]. The most commonly used inhibitors are formulated on the basis of nitrite ions. It has been proposed that these ions react with ferrous ions generating a Fe_2O_3 protective layer, thus behaving as anodic inhibitors and decreasing corrosion rates [5,6]. However, when the surface is already passive, inadequate dosages of nitrite ions could enhance the risk of pitting [2,4,7].

When the passive state can be compromised due to the presence of chlorides, the corrosion risk is determined by the chloride content, usually evaluated as the chloride/hydroxyl ratio [8]. On the other hand, the efficiency of nitrite as inhibiting agent in the presence of chloride is evaluated in terms of the nitrite/chloride ratio. There is no clear agreement on the threshold value of

* Corresponding author. Tel.: +54 223 481 6600; fax: +54 223 481 0046.
E-mail address: mvazquez@fi.mdp.edu.ar (M. Vázquez).
[1] ISE active member.

0013-4686/$ – see front matter © 2008 Elsevier Ltd. All rights reserved.
doi:10.1016/j.electacta.2008.01.091

this ratio. Different authors [2,4,9,10] have given values ranging from 0.34 to more than 1 as those necessary to prevent corrosion in concrete.

The corrosion of steel in concrete is difficult to investigate, mainly because of experimental problems such as high resistivities, highly porous materials, cell design and macrocells. An alternative way of tackling the problem is to use solutions that simulate the chemical environment present in the concrete pores. In this way, many investigations have been carried out in $Ca(OH)_2$ saturated solutions. However, the composition of concrete is much more complex [11,12]. Even when the results cannot be directly extrapolated to the situation in concrete, employing alkaline solutions is certainly a way of approaching the system, which has been extensively used [8,13–17], mainly because one is able to modify the relevant parameters one at a time.

The purpose of this investigation is to study the effect of nitrite ions on the breakdown of passive films formed on steel rebars in a highly alkaline electrolyte that simulates the solution present in chloride-contaminated concrete pores. It is our intention then, to evaluate if nitrite-base inhibitors can be helpful in controlling localized corrosion in good quality concrete prepared with contaminated aggregates. This condition will be used as reference for a work in progress where we are simulating the case of low quality concrete, where alkalinity is reduced due to the access of carbon dioxide through the concrete pores [18,19].

2. Experimental

2.1. Electrolyte composition

The experiments were carried out using an alkaline solution (AS). The composition of the AS was chosen to be KOH 0.6 mol l^{-1}, NaOH 0.2 mol l^{-1} and $Ca(OH)_2$ 0.01 mol l^{-1} with a resulting pH value of 13.9. This solution has been used before to simulate the electrolyte contained in concrete pores [20].

To evaluate the inhibitor effect, various concentrations of $NaNO_2$ (0.2, 0.4, 0.6 and 0.8 mol l^{-1}) were added to the alkaline solution where indicated.

To simulate a concrete contaminated with chloride ions, AS solutions incorporate 0.8 mol l^{-1} NaCl where indicated.

2.2. Electrodes preparation

Samples were prepared from steel reinforcement bars (Mn 0.635%, C 0.299%, Si 0.258%, Cu 0.227% and others impurities 0.245%). They were cut into disks with an area of 0.214 cm^2, provided with an electrical contact and embedded in Teflon bodies. The resulting electrodes were polished down to grade 1000 with emery paper. They were rinsed with distilled water prior to performing electrochemical measurements.

On the other hand, coupons with an area of 7.22 cm^2 were prepared and also polished down to grade 120 with emery paper. When used for electrochemical determinations, the coupons were held conveniently and the electrochemical cell was used with a fixed volume to guarantee a constant exposed area of 5.45 cm^2.

2.3. Weight loss determinations

Weight Loss Method was applied following the guidelines in ASTM D 2688 Standard Test Methods for Corrosivity of Water in the Absence of Heat Transfer. Previously weighted coupons were suspended and immersed in each testing solution, placing five coupons in each of ten containers. The metal samples were polished down to grade 120 with emery paper. The containers were kept at room temperature, with gentle agitation to avoid differential deaeration. Some coupons were withdrawn for each container after 90 days and the corrosion products were stripped by immersion in HCl 10%. Then they were neutralized with saturated Na_2CO_3 solution, and finally rinsed with distilled water. The clean and dry coupons were weighted and observed with a metallographic microscope.

The remaining coupons were employed for electrochemical tests.

2.4. Electrochemical techniques

A three-electrode electrochemical cell was used. A Hg/HgO electrode with 1 mol l^{-1} KOH solution (labelled as MOE, $E = 0.123$ V vs. NHE) was used as reference. All the potentials are indicated against this electrode. A platinum wire of large area was used as counter electrode.

All the experiments were carried out with a Voltalab PGP 201 potentiostat.

Cyclic voltammograms were recorded after deaerating the electrolyte by bubbling N_2 during 15 min prior to each measurement. The electrodes were pre-reduced at −1.1 V for 5 min. Finally the scan was started at −1.1 V and reversed at 0.50 V or at convenient potential values, as indicated. The sweep rate used was 1×10^{-2} V s^{-1}.

The open circuit potential (OCP) was measured during 24 h in the different conditions investigated.

Polarization resistance (Rp) was evaluated as $\Delta V/\Delta j$, from potential sweeps scanning ±0.01 V from the OCP at a scan rate of 1×10^{-4} V s^{-1}. Average values of over five individual experiments were obtained in the case of samples aged for 1 day, while duplicates were evaluated for coupons immersed during 90 days.

Corrosion rate, in terms of corrosion current density, can be evaluated from the polarization resistance data according to the Stern–Geary relationship as [21]:

$$j_{\mathrm{corr}} = \frac{\beta_a \beta_c}{2.303(\beta_a + \beta_c)} \frac{1}{\mathrm{Rp}} = \frac{B}{\mathrm{Rp}} \tag{1}$$

where β_a and β_c are the anodic and cathodic Tafel slopes, respectively. These are kinetic parameters characteristic of each metal–solution system.

Assuming uniform corrosion on the entire metallic surface, the nominal value of corrosion rate (CR) in μm $year^{-1}$ can be calculated using Faraday's law as:

$$\mathrm{CR} = \frac{K a_W}{n F \delta} j_{\mathrm{corr}} = \alpha j_{\mathrm{corr}} \tag{2}$$

where $K = 315{,}360$ is a units conversion factor, F the Faraday constant ($F = 96485\ \mathrm{C\,mol^{-1}}$), n the number of moles of electrons transferred, a_w the atomic weight in grams, δ the density of the metal in $\mathrm{g\,cm^{-3}}$, and j_{corr} is the current density in $\mu\mathrm{A\,cm^{-2}}$. Therefore, the value of the constant α for steel is $\alpha_{Fe} = 11.6\ \mu\mathrm{A^{-1}\,cm^2\,(m\,year^{-1}}$.

The anodic and cathodic Tafel slopes were measured from polarization curves recorded on aged electrodes, at the OCP. Anodic and cathodic polarization curves started at OCP and were recorded at $1 \times 10^{-4}\ \mathrm{V\,s^{-1}}$ in independent experiments.

When anodic polarization curves were registered using coupons with 90 days of ageing, the scan direction was reversed at $1 \times 10^{-4}\ \mathrm{A\,cm^{-2}}$. This value was chosen to induce a convenient degree of attack. The overall procedure follows the recommendations of ASTM [22].

2.5. Electrochemical impedance spectroscopy

Electrochemical impedance spectroscopy (EIS) tests were performed at open circuit potential. Recording each spectrum took between 90 and 160 min. Prior to starting the frequency sweep, the samples were kept during 90 days in contact with the test solution. The solution was used without stirring or deaereation. The amplitude of the ac voltage signal was ±0.01 V while the frequency varied between 20 kHz and 1 mHz. The results were analyzed using the equivalent circuit presented in Fig. 1. This circuit is typical of oxide-coated metals and has been used before by other authors [23,24]. The experimental data were fitted to the proposed equivalent circuit using ZView™ [25]. Corroding electrodes can show various types of inhomogeneities, which can be represented by the inclusion of constant phase elements (CPE) replacing the capacitors in the equivalent circuit. Surface roughness, insufficient polishing, grain boundaries and surface impurities had been mentioned before among the main reasons allowing the use of CPEs in equivalent circuits of corroding electrodes [26]. The impedance of this element is frequency-dependent, and can be mathematically expressed using two parameters, Q and n as:

$$Z_{CPE} = [Q(j\omega)n]^{-1} \quad (3)$$

where Q is a constant with dimensions of $\Omega\,\mathrm{cm^2\,s^{-(1-n)}}$ and n a constant power, with $-1 < n < 1$. According to the value of n, Eq. (3) accounts for an inductance ($n = -1$), a resistance ($n = 0$), a Warburg impedance ($n = 0.5$) or a capacitance ($n = 1$). A rough or porous surface can cause a double layer capacitance to appear as a constant phase element with n varying between 0.5 and 1.

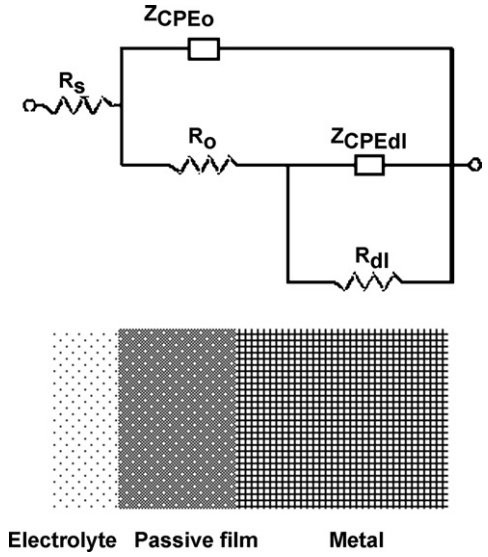

Fig. 1. Equivalent circuit proposed to fit the experimental data.

3. Results and discussion

3.1. Effect of incorporating chloride ions as contaminants (AS + Cl⁻)

The cyclic voltammogram of steel in contact with deaerated AS is shown in Fig. 2. Oxide growth starts at potentials positive to −1.10 V. A sharp anodic peak (Ia) is evident at −0.72 V, together with a shoulder at −0.36 V (IIa). There is no evidence of localized corrosion. The processes associated to the anodic peaks can be attributed to compounds containing Fe(III) such as Fe_3O_4 and δ-FeOOH, as reported before [27,28]. Various experiments carried out changing the positive limit of the potential scan showed that both anodic processes are associated to a single cathodic peak (Ic) at −0.98 V.

The detrimental effect of chloride ions to the passive layer naturally formed on iron exposed to alkaline environments has been extensively reported in the literature. Many authors have investigated the chloride threshold values for the corrosion of steel in concrete, mortars and alkaline solutions [8,16,27,29,30]. In alkaline solutions the threshold value relative to the OH^- content, given as $[Cl^-]/[OH^-]$ ratio presents a mean value around 0.6 [31,32].

Thus, a sequence of voltammograms was carried out in a solution contaminated with varying amounts of chloride ions. Low chloride concentrations such as 0.1 and $0.5\ \mathrm{mol\,l^{-1}}$ ($[Cl^-]/[OH^-] = 0.125$ and 0.625, respectively) pro-

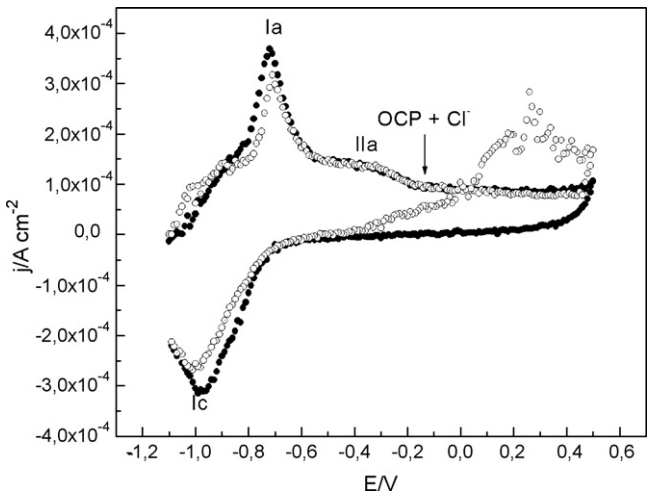

Fig. 2. Cyclic voltammogram of carbon steel in deaerated AS (●) and AS + 0.8 mol l⁻¹ NaCl (◯). Scan rate: $1 \times 10^{-2}\ \mathrm{V\,s^{-1}}$.

duced no significant differences in the voltammograms when they were compared with those in alkaline solutions free of chloride ions (AS). So, a condition where $[Cl^-]/[OH^-] = 1$ ($[NaCl] = 0.8\ mol\ l^{-1}$) was chosen to work with because the differences between AS and AS + Cl^- became clearer.

The cyclic voltammogram of steel in contact with deaerated AS + Cl^- compared with that obtained in AS is shown in Fig. 2. Both, in the AS with and without Cl^-, OCP values stabilize at around −0.15 V after 24 h of immersion, as indicated in Fig. 2. The anodic current that can be read in the voltammogram when the potential equals the OCP value is smaller than 1 mA cm^{-2}, which is typical of a metal in a passive state [27]. In the contaminated solution it can be seen that pitting starts when the potential exceeds 0.45 V, revealed by the typical hysteresis of the curve. The presence of pitting was confirmed by visual inspection of the specimens.

Anodic and cathodic polarization curves registered after 1 and 90 days of immersion are presented in Fig. 3. After 90 days of ageing, the anodic polarization curve showed pitting at potentials higher than 0.60 V. The repassivation of the surface was not possible even at OCP.

The influence of Cl^- ions on the passivity breakdown of carbon steel can be interpreted as a balance between two processes competing on the metal surface: stabilization of the passive film by OH^- adsorption and disruption of the film by Cl^- ions adsorption. When the activity of chlorides overcomes that of hydroxyls, pitting occurs [8,27].

Inside the pit, the reversible formation of Fe(OH) adsorbed on the bare metal is the first stage of the repassivation process followed by the oxidation of this layer to produce a thicker oxide film (passivating film) [33,34] according to the following sequence

$$Fe + OH^- = FeOH^-{}_{ad} \quad (1)$$

$$FeOH^-{}_{ad} = FeOH_{ad} + e^- \quad (2)$$

$$FeOH_{ad} + OH^- = Fe(OH)_{2\,s} + e^- \quad (3)$$

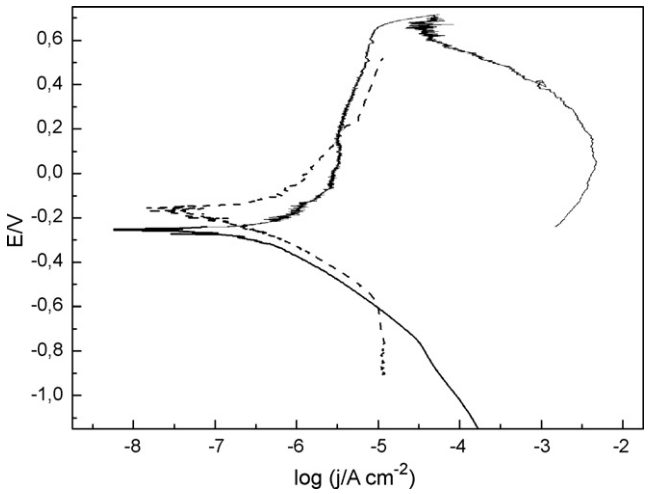

Fig. 3. Anodic and cathodic polarization curves for carbon steel in AS + 0.8 mol l^{-1} NaCl. The curves were recorded after holding the electrodes 1 (- - -) and 90 (—) days at OCP and each started at OCP. Scan rate: 1×10^{-4} V s^{-1}.

Table 1
Tafel slopes evaluated from the linear portion of the polarization curves (Figs. 3 and 6): $B = \beta_a\beta_c/2.303(\beta_a + \beta_c)$

Electrolyte	1 day			90 days		
	β_a (V)	β_c (V)	B (V)	β_a(V)	β_c (V)	B (V)
AS + Cl^-	0.240	0.167	0.043	0.187	0.191	0.041
AS + Cl^- + NO_2^-	0.327	0.180	0.050	0.216	0.160	0.040

$$Fe(OH)_{2\,s} + OH^- \rightarrow FeOOH_s + H_2O + e^- \quad (4)$$

In the presence of chloride ions, the $Fe(OH)_{ad}$ coverage decreases resulting in an increasing of the anodic dissolution of the metal, when the following reactions occur

$$Fe + Cl^- = FeCl_{ad} + e^- \quad (5)$$

$$FeCl_{ad} = FeCl^+{}_{aq} + e^- \quad (6)$$

The Tafel slopes were measured from anodic and cathodic polarization curves between ±60 to 120 mV from the OCP and the corresponding B values, calculated using Eq. (1) are summarized in Table 1. Based on polarization resistance and gravimetric measurements, Andrade and coworkers [35] reported typical values of B for steel embedded in mortar. According to them, the value of B for bare steel in the passive state is 0.052 V while in the active state the corresponding value of B is 0.026 V. Taking into account that our work is carried out in an alkaline solution, the values calculated for the parameter B in Table 1 are in good agreement with passive steel. From these values, the corrosion current density can be calculated applying Eq. (1), while the corrosion rate can be calculated by means of Eq. (2). The j_{corr} and CR values are presented in Table 2.

The same parameters were calculated by EIS. The results of the impedance spectra recorded using steel electrodes aged during 90 days are shown in Fig. 4 in the form of Nyquist and Bode plots. As can be seen, the spectra present two time constants. EIS data were fitted using the equivalent circuit shown in Fig. 1. R_s represents the solutions resistance, Q_0 a constant related to the surface oxide, R_0 the resistance to current flow through defects in the surface oxide, Q_{dl} a constant related to the double layer and R_{dl} the polarization resistance. The fit is also shown in Fig. 4, together with the recorded data. The experimental data were found to be sufficiently well fitted by the proposed equivalent

Table 2
Corrosion current density and corrosion rate for carbon steel aged at OCP

	By sweep 1 day	By sweep 90 days	By impedance 90 days
AS + Cl^-			
j_{corr} (A cm^{-2})	2×10^{-7}	4.5×10^{-7}	4.3×10^{-7}
CR (μm $year^{-1}$)	2.3	5.2	5.0
AS + Cl^- + NO_2^-			
j_{corr} (A cm^{-2})	2.1×10^{-7}	4.3×10^{-7}	5.1×10^{-7}
CR (μm $year^{-1}$)	2.4	6.5	7.7

"By impedance" values are calculated after fitting EIS results with the equivalent circuit in Fig. 1. "By sweep" values are calculated from the polarization resistance measurements.

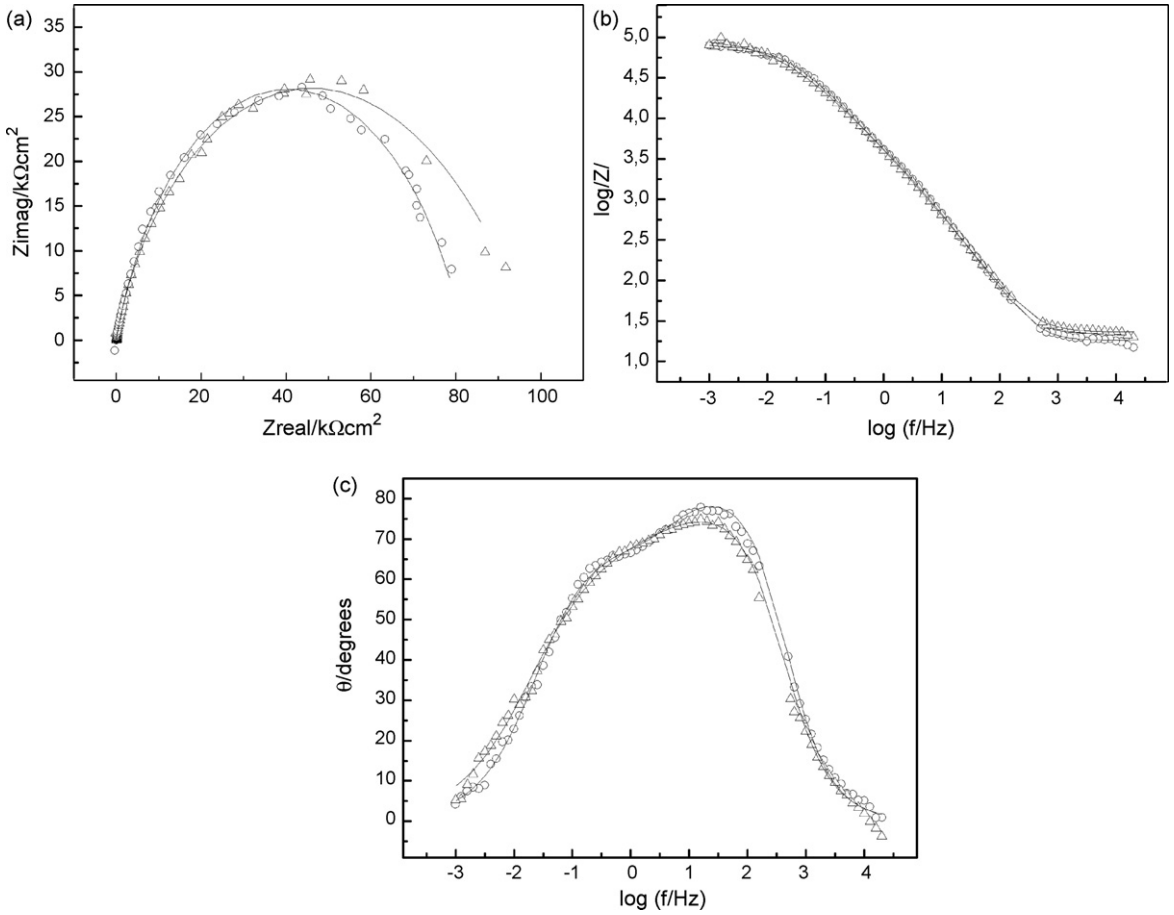

Fig. 4. Impedance spectra recorded on carbon steel electrodes held for 90 days at OCP in AS + Cl^- (Δ) and AS + Cl^- + NO_2^- (◯). The symbols represent the data and the lines the fitting results. (a) Nyquist representation; (b) and (c) Bode representation.

circuit. The values for the various parameters are presented in Table 3. The corrosion current density and corrosion rate was calculated taking R_{dl} as the charge transfer resistance and using Eqs. (1) and (2).

The results presented in Table 2 show that the j_{corr} values agree well with those calculated by polarizing the electrode and calculating Rp in the more conventional way.

Many authors have used equivalent circuits containing two time constants to successfully analyze results for steel in alkaline electrolytes [36–39], either in parallel or series configurations.

In highly alkaline solutions, the typical j_{corr} values of passive steel are close to 2×10^{-7} A cm^{-2} [14,17], while values higher than 1×10^{-6} A cm^{-2} are typical of the active state [16,40]. In AS + Cl^- after 1 day of ageing the steel surface is passive, as well as after 90 days of ageing. The CR values measured in AS + Cl^- are in agreement with values reported in the literature, measured in similar conditions [41].

The weight loss registered in the coupons after an immersion period of 90 days was negligible. This would indicate that a very compact and adherent passive film forms at open circuit potential, which was not possible to remove by chemical cleaning. Also, no particular features were revealed upon examination of the metallic surface with an optical microscope, reconfirming that the metallic surface is passive. These specimens will serve as blanks when evaluating the effect of nitrite ions in Sections 3.2 and 3.3. Nevertheless, a "true" blank sample was immersed just in AS for the sake of comparison and showed no difference.

Table 3
Optimised parameters fitting the data in Fig. 4 to the equivalent circuit in Fig. 1

Element	AS + Cl^-	AS + Cl^- + NO_2^-
R_s (Ω cm^2)	23	18
Q_0 (Ω^{-1} cm^{-2} S^N)	3.47×10^{-5}	2.83×10^{-5}
n_0	0.90	0.95
R_0 (Ω cm^2)	3168	3896
Q_{dl} (Ω^{-1} cm^{-2} S^N)	3.29×10^{-5}	3.60×10^{-5}
n_{dl}	0.56	0.68
R_{dl} (Ω cm^2)	95261	78441

3.2. *Effect of incorporating chloride ions as contaminants together with nitrite ions as inhibitors (AS + Cl^- + NO_2^-)*

A sequence of experiments similar to that reported in Section 3.1 was carried out in a solution that incorporates both chloride and nitrite ions.

The nitrite ions concentration was chosen on the basis of the results of Li et al. [42] and Berke and Hicks [10]. Li et al. have used an *in-situ* leaching technique to provide representative estimates of the nitrite concentration in pore solution, establishing a value of 8000 ppm (equivalent to 0.17 mol l^{-1}) as

typical. This concrete was produced incorporating 22 l m^{-3} of 30% $Ca(NO_2)_2$ to concrete with 0.4 water/cement. Later, Berke et al. have recommended the addition of 15–30 l m^{-3} of 30% $Ca(NO_2)_2$ to concrete with 0.4 water/cement, in order to extend severe corrosion initiation times up to 50 years. From this information, 0.2 mol l^{-1} nitrite was the selected concentration, so that $[NO_2^-]/[Cl^-] = 0.25$.

The cyclic voltammogram of steel in contact with deaerated AS + Cl^- + NO_2^- is shown in Fig. 5 compared to that obtained in AS. Again, just one main anodic peak is present with a current maximum at a potential similar to that registered in the absence of inhibitor. The total current is also similar but slightly higher, and this can be associated to redox processes involving the reduction of NO_2^- to N_2O. This is particularly the case in the most negative potentials.

In this electrolyte, OCP values stabilize at around −0.07 V after 24 h of immersion. No big difference is apparent between this value and those registered in the absence of nitrites. Again, when reading the current in the voltammogram at the OCP, the anodic current is lower than 1 mA cm^{-2}.

Anodic and cathodic polarization curves registered after 1 and 90 days of immersion are presented in Fig. 6. After 90 days of ageing, the anodic polarization curve showed pitting at potentials positive to 0.60 V. Due to the presence of nitrite ions in the electrolyte, repassivation starts as soon as the potential sweep is reverted. The inhibition of pit growth has been explained in terms of hard and soft acids and bases principle (HSAB) [43]. Within this framework, NO_2^- is acting as a soft base by chemisorpting on the bare iron substrate, displacing chloride ions inside the pit. The presence of nitrite ions could favor the oxidation process [19] according to reactions 1–4, following a processes that can be summarized as

$$4Fe(OH)_{2\,s} + 2NO_2^- \rightarrow N_2O + 4FeOOH_s + HO^- + H_2O \quad (7)$$

The Tafel slopes and the corresponding B values, calculated using Eq. (1) are summarized in Table 1. The j_{corr} and CR values are presented in Table 2.

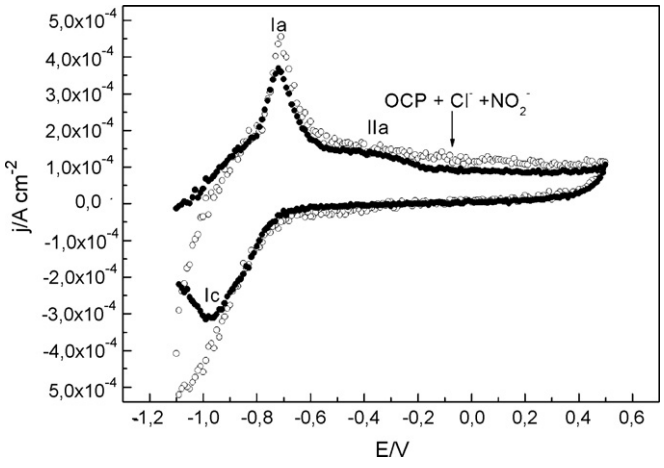

Fig. 5. Cyclic voltammograms of carbon steel in deaerated AS (●) and AS + Cl^- + NO_2^- (◯). Scan rate: 1 × 10^{-2} V s^{-1}.

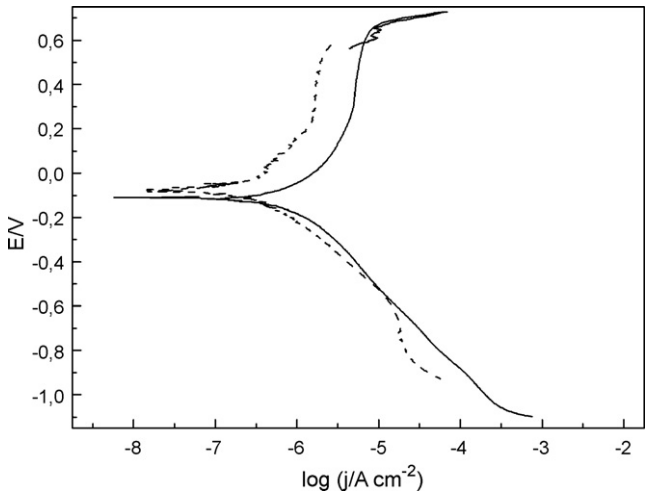

Fig. 6. Anodic and cathodic polarization curves for carbon steel in AS + Cl^- + NO_2^-. The curves were recorded after holding the electrodes 1 (- - -) and 90 (—) days at OCP and each started at OCP. Scan rate: 1 × 10^{-4} V s^{-1}.

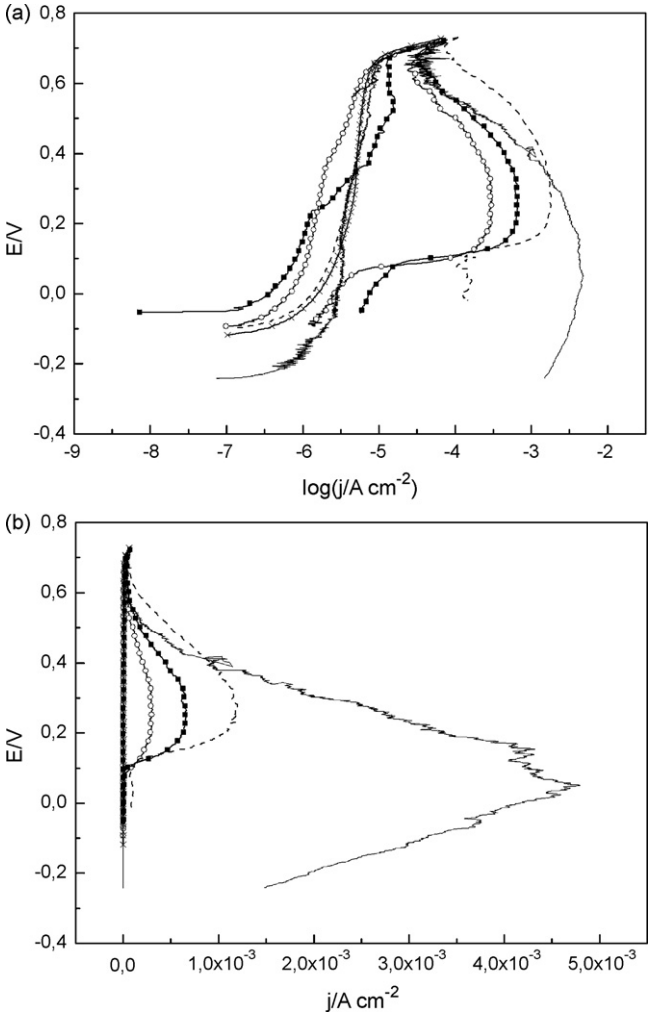

Fig. 7. Anodic polarization curves for carbon steel in SPS with different nitrite to chloride ratios in (a) logarithmic scale and (b) normal scale. AS + Cl^- (—), AS + Cl^- + NO_2^- ($[NO_2^-]/[Cl^-] = 0.25$) (×), AS + Cl^- + 0.4 mol l^{-1} $NaNO_2$ ($[NO_2^-]/[Cl^-] = 0.5$) (◯), AS + Cl^- + 0.6 mol l^{-1} $NaNO_2$ ($[NO_2^-]/[Cl^-] = 0.75$) (■) and AS + Cl^- + 0.8 mol l^{-1} $NaNO_2$ ($[NO_2^-]/[Cl^-] = 1$) (– – –). The curves were recorded after holding the electrodes 90 days at OCP and each started at OCP. Scan rate: 1 × 10^{-4} V s^{-1}.

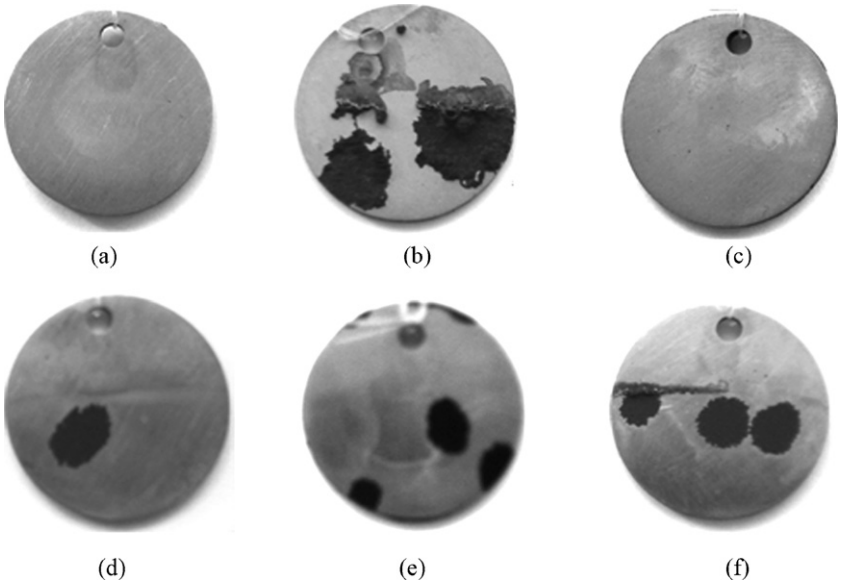

Fig. 8. Photographs of coupons after performing anodic polarization curves. (a) AS, (b) $AS + Cl^-$, (c) $AS + Cl^- + NO_2^-$ ($[NO_2^-]/[Cl^-] = 0.25$), (d) $AS + Cl^- + 0.4\,mol\,l^{-1}$ $NaNO_2$ ($[NO_2^-]/[Cl^-] = 0.5$), (e) $AS + Cl^- + 0.6\,mol\,l^{-1}$ $NaNO_2$ ($[NO_2^-]/[Cl^-] = 0.75$) and (f) $AS + Cl^- + 0.8\,mol\,l^{-1}$ $NaNO_2$ ($[NO_2^-]/[Cl^-] = 1$).

No significant differences in the cathodic Tafel slopes were observed when the inhibitor was incorporated. Thus, the inhibitor does not seem to influence the mechanism of the cathodic reaction [44].

The impedance spectra recorded using electrodes aged during 90 days are shown in Fig. 4 in the form of Nyquist and Bode plots. Again, the impedance spectra were fitted using the equivalent circuit in Fig. 1. The values for the various parameters are presented in Table 3. Values of n_0 close to 0.9 are typical of porous film [45,46]. As can be seen, Q_0 and R_0 did not show significant differences when nitrites ions are added to the test solution, indicating that no changes occur in the density or thickness of the passive layer.

The corrosion current density and corrosion rate was calculated using Eqs. (1) and (3). The results are shown in Table 2. Both, the j_{corr} and CR values showed no significant differences when compared to values measured in the absence of nitrite ions.

The weight loss registered in the coupons after an immersion period of 90 days was negligible and no particular features were revealed with microscopic examination.

3.3. Effect of varying the inhibitor concentration

The effect of varying the nitrite dosage was evaluated comparing the anodic polarization curves performed on samples aged for 90 days. Coupons were immersed in alkaline solutions with a chloride concentration of $0.8\,mol\,l^{-1}$ and nitrite/chloride ratios of 0, 0.25, 0.5, 0.75 and 1.

The direction of the potential sweep was reversed at a predetermined current density value, in order to make the visual comparison of the surfaces more significant. The anodic polarization curves are presented in Fig. 7a and b.

Fig. 8 shows photographs of the coupons after performing the anodic polarization curves. When observed at the microscope, the samples in contact with $AS + Cl^-$ presented the highest density of pits, which are also bigger and deeper. In the presence of varying amounts of nitrites, the degree of attack decreases as the nitrite content decreases, and when $[NO_2^-]/[Cl^-] = 0.25$, the localized attack is minimal (see Fig. 9).

From Fig. 7a and b passivity currents (j_a), pitting potentials (E_{pit}) and repassivation potentials (E_{rp}), together with the maximum current after reversing the sweep (j_b) were evaluated. Some

Table 4
Relevant electrochemical parameters, characteristic of the anodic polarization curves in carbon steel after 90 days of immersion

	NO_2^-/Cl^- ratio				
	0	0.25	0.5	0.75	1
E_{corr} (V)	−0.240	−0.112	−0.105	−0.049	−0.109
j_a ($A\,cm^{-2}$)	4.6×10^{-6}	5.2×10^{-6}	2.0×10^{-6}	3.6×10^{-6}	4.5×10^{-6}
E_{rp} (V)	–	0.585	–	–	–
j_b ($A\,cm^{-2}$)	4.8×10^{-2}	3.5×10^{-6}	3.0×10^{-4}	7.0×10^{-4}	1.0×10^{-3}
j_c ($A\,cm^{-2}$)	1.5×10^{-3}	5.0×10^{-6}	1.4×10^{-6}	1.5×10^{-5}	1.4×10^{-4}

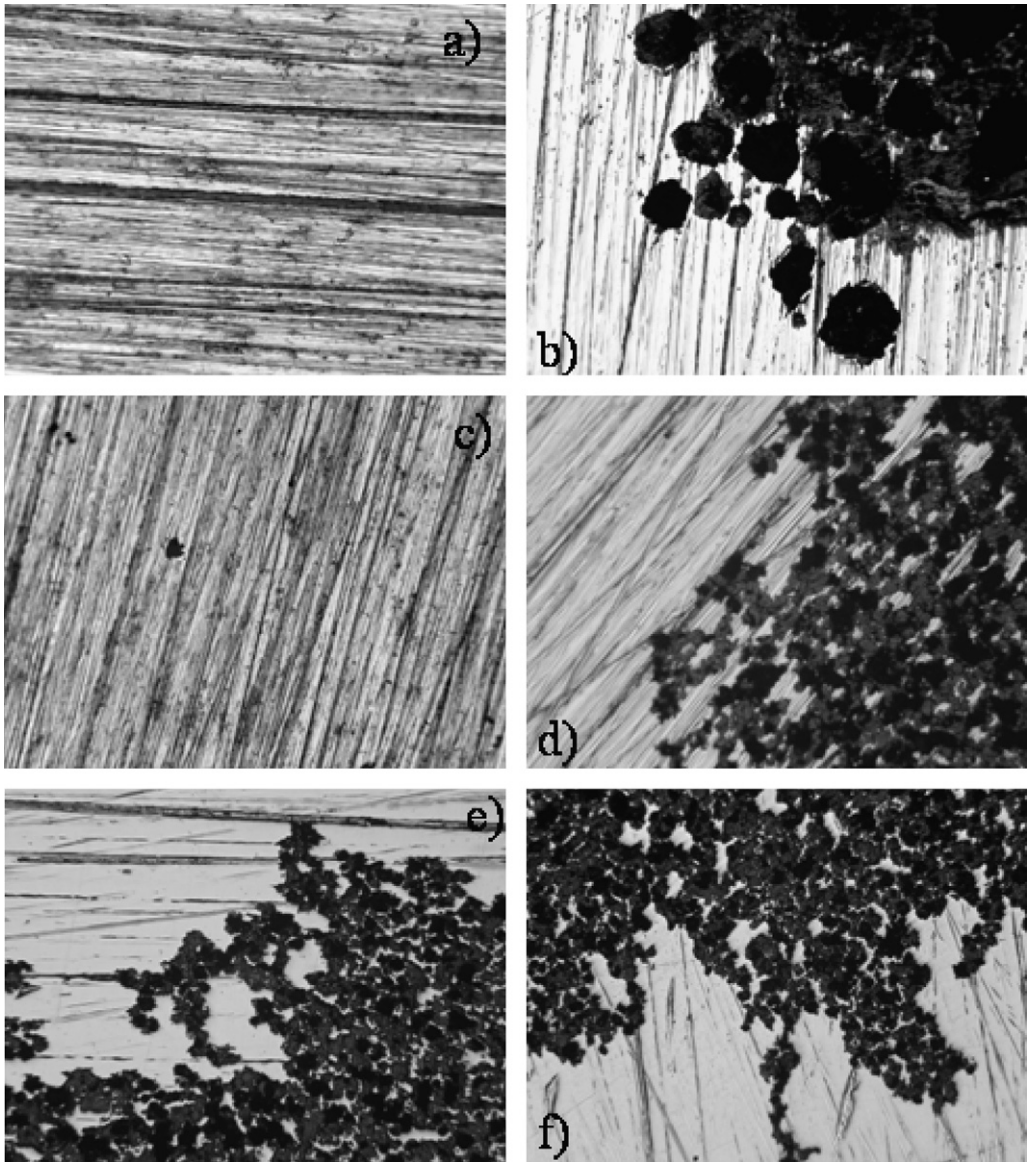

Fig. 9. Micrographs (100×) of coupons surface after performing anodic polarization curves. (a) AS, (b) AS + Cl^-, (c) AS + Cl^- + NO_2^- ($[NO_2^-]/[Cl^-] = 0.25$), (d) AS + Cl^- + 0.4 mol l^{-1} $NaNO_2$ ($[NO_2^-]/[Cl^-] = 0.5$), (e) AS + Cl^- + 0.6 mol l^{-1} $NaNO_2$ ($[NO_2^-]/[Cl^-] = 0.75$) and (f) AS + Cl^- + 0.8 mol l^{-1} $NaNO_2$ ($[NO_2^-]/[Cl^-] = 1$).

of these values are presented in Table 4. After reversing the sweep, the currents measured when the electrode reaches the open circuit potential (as measured before polarizing), labeled j_c, are also presented in Table 4.

The passivity currents, measured in all the different conditions, did not show important differences. Pitting was only observed when potentials were higher than 0.60 V, independently of the $[NO_2^-]/[Cl^-]$ ratio. However, only when $[NO_2^-]/[Cl^-] = 0.25$ (Fig. 7a) was the surface repassivation possible. The hysteresis area is also the smallest and the pitting resistance of the metal seems to improve. On the other hand, when higher $[NO_2^-]/[Cl^-]$ ratios were used, there was no repassivation in the strict sense of currents cross-over, even at the open circuit potential. However, j_c is always lower when nitrite ions are present, even though increasing slightly as the nitrite content increases.

As expected, the maximum current after reversing the sweep (j_b) reaches its maximum value in the absence of nitrite ions (Fig. 7b). It has to be taken into account that j_b represents the rate of metal dissolution within the pits [8,47]. But surprisingly, in the presence of nitrite ions, j_b increased as the nitrite/chloride ratio increased.

If the inhibitor hinders pit growth by selective adsorption on the iron surface within the pit, the current density of iron dissolution (j_b) should decrease when it is present. However, the inhibiting effect of nitrites on pitting in polluted alkaline solutions seems to have a non-linear variation with the nitrite concentration value. This can be explained on the basis of the competitive adsorption between nitrite and hydroxyl ions on the steel surface, as discussed earlier for Fe and Ni [48]. In this way at higher nitrite ions concentrations and positive imposed potentials, a competitive adsorption between NO_2^- and OH^- on the

bare metal inside the pit could decrease the amount of $Fe(OH)_{ad}$ on the surface, retarding the repassivation process (reaction 3 and 4). A similar effect was observed on Ni in the presence of nitrite ions and slightly acidic conditions [49]. The non-linear behavior of nitrite ions concentration on j_b could be explained in these terms.

4. Conclusions

At open circuit potential, carbon steel attains a very stable passive state when in contact with highly alkaline solutions, even if they are contaminated with chloride ions.

When nitrite ions are present, no changes can be observed in the composition, density or thickness of the passive layer. Even when nitrite ions do not seem to affect pit initiation in this experimental condition, they certainly behave as effective inhibitors of pit propagation for all the dosages tested. This inhibiting effect is greater when the $[NO_2^-]/[Cl^-]$ ratio is 0.25. Therefore, there seems to be no benefit in increasing the inhibitor dosages to higher values. Moreover, as the pitting potential is far from the OCP, pitting corrosion should represent no risk when steel rebars are in contact with a highly alkaline environment. When steel is in contact with an alkaline electrolyte that contains 0.8 mol/l of chloride ions and even if no inhibitor is present, no pitting was observed after 90 days of immersion at the OCP.

When the electrodes are polarized to positive potentials, the presence of chloride ions shows no effect for $[Cl^-]/[OH^-]$ ratios lower than 1. Only when the $[Cl^-]/[OH^-]$ ratio equals one, does localized attack (pitting) become evident, but the metal samples have to be polarized more than 0.6 V from OCP.

It can be concluded then, that when preparing concrete with contaminated aggregates, the passive state of steel can be guaranteed provided that good quality concrete, with low porosity and appropriated cover thicknesses maintain high pH values close to the rebars. In the event that the passive layer is damaged and pitting can be initiated, nitrite ions can help in inhibiting pit propagation. The influence of nitrite in carbonated concrete, where alkalinity can be significantly lowered, is currently under evaluation.

Acknowledgements

This work has been supported by the University of Mar del Plata (Grant 15/G150), as well as by the National Research Council (CONICET, PIP6252) and the Agencia Nacional de Promoción Científica y Tecnológica (PICTO 762/04). One of the authors (MBV) acknowledges CONICET for supporting her by means of a post-graduation scholarship.

References

[1] V.S. Sastri, Corrosion Inhibitors, West Sussex, England, 1998.
[2] C.L. Page, V.T. Ngala, M.M. Page, Mag. Concr. Res. 52 (2000) 25.
[3] C.M. Hansson, L. Mammoliti, B.B. Hope, Cem. Concr. Res. 28 (12) (1998) 1775.
[4] B. Elsener, Corrosion inhibitors for steel in concrete, State of the art report, EFC Publication 35, The Institute of Materials, Maney Publishing, London, 2001.
[5] A.M. Rosembreg, J.M. Gaidis, Mater. Performance 18 (11) (1979) 45.
[6] J.M. Gaidis, Cem. Concr. Compos. 26 (3) (2004) 181.
[7] J.A. González, E. Ramírez, A. Bautista, Cem. Concr. Res. 28 (4) (1998) 577.
[8] M. Saremi, E. Mahallati, Cem. Concr. Res. 32 (2002) 1915.
[9] K.Y. Ann, H.S. Jung, H.S. Kim, S.S. Kim, H.Y. Moon, Cem. Concr. Res. 36 (3) (2006) 530.
[10] N.S. Berke, M.C. Hicks, Cem. Concr. Comp. 26 (2004) 191.
[11] L. Veleva, M.A. Alpuche-Aviles, M.K. Graves-Brook, D.O. Wipf, J. Electroanal. Chem. 537 (2002) 85.
[12] L. Veleva, M.A. Alpuche-Aviles, M.K. Graves-Brook, D.O. Wipf, J. Electroanal. Chem. 578 (2005) 45.
[13] S. Goñi, C. Andrade, Cem. Concr. Res. 20 (4) (1990) 525.
[14] J.A. Gonzalez, E. Ramirez, A. Bautista, S. Feliu, Cem. Concr. Res. 26 (3) (1996) 501.
[15] C. Monticelli, A. Frignani, G. Trabanelli, J. Appl. Electrochem. 32 (2002) 527.
[16] M.F. Hurley, J.R. Scully, Corrosion (October) (2006) 892.
[17] A. Poursaee, C.M. Hansson, Cem. Concr. Res. 37 (2007) 1127.
[18] B. Huet, V. L'Hostis, F. Miserque, H. Idrissi, Electrochim. Acta 51 (2005) 172.
[19] M. Refass, R. Sabot, M. Jeannin, P. Refait, Electrochim. Acta 52 (27) (2007) 7599.
[20] G. Guidoni, M. Vázquez, Anti-Corros. Methods Mater. 51 (1) (2004) 18.
[21] M. Stern, A.L. Geary, J. Electrochem. Soc. 104 (1957) 56.
[22] American Society of Testing and Materials, ASTM G61-86, Philadelphia, 1993.
[23] A. Palit, S. Pehkonen, Corros. Sci. 42 (2000) 1801.
[24] J. Shim, J. Kim, Mater. Lett. 58 (2004) 2002.
[25] M. Vazquez, S.R.d. Sanchez, J. Appl. Electrochem. 28 (1998) 1383.
[26] L.J. Aljinovic, S. Gudic, M. Smith, J. Appl. Electrochem. 30 (2000) 973.
[27] F. Foulkes, P. McGrath, Cem. Concr. Res. 29 (1999) 873.
[28] S.T. Amaral, E.M.A. Martini, I.L. Muller, Corros. Sci. 43 (5) (2001) 853.
[29] C. Alonso, M. Castellote, C. Andrade, Electrochim. Acta 47 (21) (2002) 3469.
[30] C. Alonso, C. Andrade, M. Castellote, P. Castro, Cem. Concr. Res. 30 (7) (2000) 1047.
[31] D.A. Hausmann, J. Mater. Prot. (1967) 19.
[32] V.K. Gouda, Br. Corros. J 5 (1970) 198.
[33] A. Saraby-Reintjes, Electrochim. Acta 30 (3) (1985) 403.
[34] J.D. Kim, S.I. Pyum, Corros. Sci. 38 (7) (1996) 1093.
[35] J. Gonzalez, S. Algaba, C. Andrade, Br. Corros. J. 15 (1980) 135.
[36] C. Andrade, M. Keddam, X.R. Novoa, M.C. Perez, C.M. Rangel, H. Takenouti, Electrochim. Acta 46 (24–25) (2001) 3905.
[37] M. Ormellese, M. Berra, F. Bolzoni, T. Pastore, Cem. Concr. Res. 36 (3) (2006) 536.
[38] C.M. Abreu, M.J. Cristóbal, R. Losada, X.R. Nóvoa, G. Pena, M.C. Pérez, J. Electroanal. Chem. 572 (2004) 335.
[39] G. Blanco, A. Bautista, H. Takenouti, Cem. Concr. Res. 28 (2006) 212.
[40] J.A. Gonzalez, J.M. Miranda, N. Birbilis, S. Feliu, Corrosion 61 (1) (2005) 37.
[41] C. Monticelli, A. Frignani, G. Trabanelli, J. Appl. Electrochem. 30 (4) (2000) 635.
[42] L. Li, A.A. Sagues, N. Poor, Cem. Concr. Res. 29 (3) (1999) 315.
[43] M. Yamaguchi, H. Nishihara, K. Aramaki, Corros. Sci. 37 (4) (1995) 571.
[44] L.L. Shreir, R.A. Jarman, G.T. Burstein, Corrosion Control, vol. 2, Oxford, UK, 1995.
[45] S. Associates, 1998, Cap. 8, p. 16.
[46] M.E. Folquer, S.B. Ribotta, S.G. Real, L.M. Gassa, Corrosion 58 (3) (2002) 240.
[47] E. Fujioka, H. Nishihara, K. Aramaki, Corros. Sci. 38 (11) (1996) 1915.
[48] S.A.M. Refaey, S.S.A. El-Rehim, F. Taha, M.B. Saleh, R.A. Ahmed, Appl. Surf. Sci. 158 (2000) 190.
[49] A.G. Muñoz, J.W. Schultze, Electrochim. Acta 49 (2004) 293.